Hypomorphic Pathogenic Variants in *TAF13* Are Associated with Autosomal-Recessive Intellectual Disability and Microcephaly

Hasan Tawamie,[1,2] Igor Martianov,[3] Natalie Wohlfahrt,[1] Rebecca Buchert,[4] Gabrielle Mengus,[3] Steffen Uebe,[1] Luigi Janiri,[5] Franz Wolfgang Hirsch,[6] Johannes Schumacher,[7] Fulvia Ferrazzi,[1] Heinrich Sticht,[8] André Reis,[1] Irwin Davidson,[3] Roberto Colombo,[9,10] and Rami Abou Jamra[1,2,*]

In two independent consanguineous families each with two children affected by mild intellectual disability and microcephaly, we identified two homozygous missense variants (c.119T>A [p.Met40Lys] and c.92T>A [p.Leu31His]) in TATA-box-binding-protein-associated factor 13 (*TAF13*). Molecular modeling suggested a pathogenic effect of both variants through disruption of the interaction between TAF13 and TAF11. These two proteins form a histone-like heterodimer that is essential for their recruitment into the general RNA polymerase II transcription factor IID (TFIID) complex. Co-immunoprecipitation in HeLa cells transfected with plasmids encoding TAF11 and TAF13 revealed that both variants indeed impaired formation of the TAF13-TAF11 heterodimer, thus confirming the protein modeling analysis. To further understand the functional role of TAF13, we performed RNA sequencing of neuroblastoma cell lines upon *TAF13* knockdown. The transcriptional profile showed significant deregulation of gene expression patterns with an emphasis on genes related to neuronal and skeletal functions and those containing E-box motives in their promoters. Here, we expand the spectrum of TAF-associated phenotypes and highlight the importance of *TAF13* in neuronal functions.

Intellectual disability (ID) is the most common reason for referral to clinical genetic centers and has a substantial impact on the affected individuals, their families, and the health system.[1] In order to illuminate the highly heterogeneous genetic causes of ID, we examined a large cohort of consanguineous families affected by probably autosomal-recessive ID.[2] To support the exchange of information between scientists, we established the Consortium of Autosomal-Recessive Intellectual Disability (CARID), which aims to facilitate the sharing of clinical and molecular data. These efforts led to the identification of two homozygous variants in TATA-box-binding-protein-associated factor 13 (*TAF13* [MIM: 600774]) that co-segregate with ID in two independent families.

TAF13 forms a histone-fold-like heterodimer with TAF11, and this heterodimer is essential for their recruitment into the RNA polymerase II general transcription factor IID (TFIID) protein complex.[3–6] TFIID is an essential component of the RNA polymerase II pre-initiation complex and is composed of TBP and 13–14 evolutionarily conserved TBP-associated factors (TAFs), which specifically interact with a variety of core promoter DNA sequences. TFIID plays a central role in forming the pre-initiation complex (PIC) by providing an interface for other PIC components, such as TFIIA and TFIIB, the recognition of core promoter DNA elements such as the TATA and downstream promoter elements, and interactions with modified histone tails and transcriptional activators.[7] Pathogenic variants associated with neurological phenotypes have been reported in several components of the TFIID complex. Mutations in *TAF1* (MIM: 313650) and TATA-box-binding protein (*TBP* [MIM: 600075]) are associated with X-linked dystonia-parkinsonism (XDP [MIM: 314250]) and spinocerebellar ataxia 17 (SCA17 [MIM: 607136]), respectively. Variants in *TAF1*, *TBP*, and *TAF2* (MIM: 604912) have been reported in individuals with ID. Recently, pathogenic variants in *TAF6* (MIM: 602955) have also been suggested to play an important role in the pathogenesis of an autosomal-recessive disorder resembling Cornelia de Lange syndrome (MIM: 122470, 300590, 610759, 614701, and 300882;[8–15] overview in Table S1). However, still little is known about the functions of TAFs in CNS development and diseases.

We clinically examined two families and obtained their approval to be included in a research study. The study protocol was approved by the ethics committees of the Universities of Bonn and Erlangen-Nürnberg (Germany) and is in agreement with the guidelines for biomedical research on human subjects issued by the ethics committee of the Catholic University (Rome). Written informed consent was obtained from all examined individuals or their guardians.

Family 1 is of Syrian Kurdish descent. The parents are first cousins and had six children (Figure 1), one of

[1]Institute of Human Genetics, Friedrich-Alexander-Universität Erlangen-Nürnberg, 91054 Erlangen, Germany; [2]Institute of Human Genetics, University Medical Center Leipzig, 04103 Leipzig, Germany; [3]Institut de Génétique et de Biologie Moléculaire et Cellulaire, 67404 Illkirch Cedex, France; [4]Institute of Medical Genetics and Applied Genomics, University of Tübingen, 72076 Tübingen, Germany; [5]Institute of Psychiatry and Psychology, Faculty of Medicine, Catholic University of Sacred Heart, 00168 Rome, Italy; [6]Section of Pediatric Radiology, Department of Imaging, University Medical Center Leipzig, 04103 Leipzig, Germany; [7]Institute of Human Genetics, University of Bonn, 53127 Bonn, Germany; [8]Bioinformatics, Institute of Biochemistry, Friedrich-Alexander-Universität Erlangen-Nürnberg, 91054 Erlangen, Germany; [9]Institute of Clinical Biochemistry, Faculty of Medicine, Catholic University of Sacred Heart, 00168 Rome, Italy; [10]Center for the Study of Rare Hereditary Diseases, Niguarda Ca' Granda Metropolitan Hospital, 20162 Milan, Italy
*Correspondence: rami.aboujamra@medizin.uni-leipzig.de
http://dx.doi.org/10.1016/j.ajhg.2017.01.032.

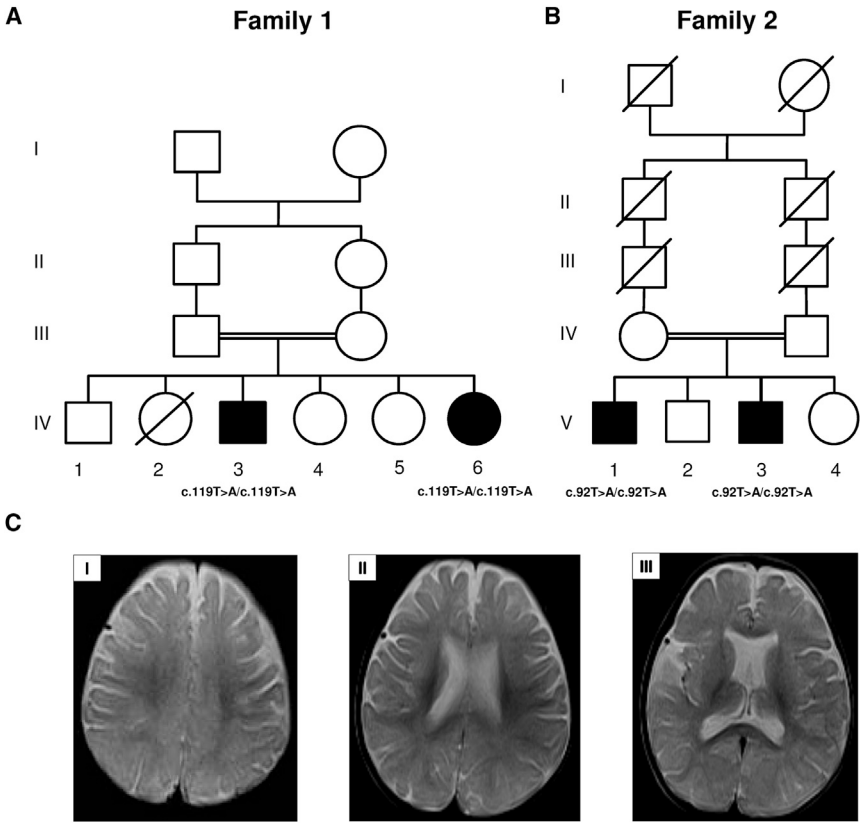

Figure 1. Pedigrees of Affected Individuals and MRI of Individual IV-6 from Family 1

(A and B) Pedigrees of families 1 (A) and 2 (B).

(C) MRI of individual IV-6 at 10 months of age shows mild delayed myelinization (I), discrete frontal pachygyria (II), and deep sulci of the cerebrum (III).

whom died 2 hours after birth as a result of multiple malformations. Of the other five children, two (IV-3 and IV-6; Figure 1) have mild ID, microcephaly, and severe growth retardation. Pregnancy and delivery of both affected siblings were normal. Low birth weight of 2 kg was noted in both (below the third percentile [−2.5 SD]; no information regarding length and head circumference). No convulsions were reported, and hearing and vision seemed normal, as was social interaction. Neither showed any malformations. The parents reported that the elder boy (IV-3) achieved all developmental milestones slightly belatedly, e.g., he walked at about 2 years. An examination at the age of 7 years revealed delayed bone at 3 years. At the time of examination, IV-3 was 16.5 years old and showed no signs of puberty. Height was 134 cm (30 cm below the third percentile [−6.07 SD]), weight was 24 kg (25 kg below the third percentile [−9.39 SD]), and head circumference was 46 cm (7.5 cm below the fifth percentile [−7.06 SD]). At the time of examination, the younger sister (IV-6) was 10 months old, and she could sit alone. Weight was 5.3 kg (1.4 kg below the third percentile [−3.57 SD]), and head circumference was 39 cm (4 cm below the third percentile [−5.83 SD]). We could not obtain a reliable measurement of her length, but she was significantly smaller than expected for her age. MRI of IV-6 at the age of 10 months revealed slightly delayed myelination (Figure 1C, I) and deep sulci of the cerebellum (Figure 1C, III), which corresponds to the brain development of a 6-month-old child and a suspected pachygyria with slightly enlarged gyri in the frontal lobe (Figure 1C, II). Genetic tests composed of karyotyping, array analyses, and screening for fragile X syndrome were normal.

Family 2 is of southern Italian origin and includes two male children (individuals V-1 and V-3; Figure 1) also presenting with mild ID and microcephaly. The parents are second cousins, and they and their other two children are all healthy. Pregnancies and deliveries of V-1 and V-3 were without complications. The older affected brother (V-1) was born at 37 weeks of gestation with a weight of 2.1 kg (below the third percentile [−1.9 SD]), length of 44 cm (second percentile [−2 SD]), and head circumference of 30 cm (first percentile [−2.4 SD]). Psychomotor development was delayed: he was able to sit without support at approximately 9 months, started walking independently at 18 months, and spoke his first words at 2 years. The boy had one febrile seizure episode at the same age and no dysmorphic facial features. The onset of puberty and bone age was delayed by 3 and 2 years, respectively. During a 3-year follow-up, his weight and head circumference were below the tenth and the fifth percentiles, respectively, and his height was at the 25th percentile. Brain computed tomography (CT) at the age of 7.5 years was normal, as were array analysis and karyotype studies. The younger affected brother (V-3) was born at 39 weeks of gestation. Birth parameters were low: weight of 2.4 kg (below the second percentile [−2.1 SD]), length of 46 cm (below the third percentile [−1.9 SD]), and head circumference of 31.5 cm (second percentile [−2 SD]). At 2.7 years of age, his height was 88 cm (tenth percentile), his weight was 11.5 kg (below the fifth percentile), and his head circumference was 46 cm (below the third percentile). He had recurrent infections of the upper airways and a single febrile seizure. The child showed global developmental delay and started walking without support shortly before the age of 2 years. He attended normal school but experienced learning and socialization difficulties as well as anxiety. Neurological examination was normal. No dysmorphic features were observed, but bone age was delayed by more than 2 years. At 12.4 years, Tanner stage was 2. Urinary ketones,

Table 1. An Overview of the Clinical Presentation of All Four Individuals with a Homozygous Variant in *TAF13* Shows a Significant Phenotypic Overlap

	Family 1		Family 2	
Symptoms	**IV-3**	**IV-6**	**V-1**	**V-3**
Pregnancy and delivery	normal	normal	normal	normal
Delay of development milestones	mild	mild	mild	mild
Intellectual disability	mild	mild	mild	mild
Dysmorphic facial features	none	none	none	none
Puberty signs	delayed	not available	delayed	delayed
Bone age	delayed	not available	delayed	delayed
Growth retardation	severe	severe	normal	normal
Microcephaly	severe	severe	moderate	mild
Brain imaging	not available	MRI showed delayed myelination	CT scan at the age of 7.5 years was unremarkable	not available

non-glucose reducing substances, organic acid and amino acid profiles, array analysis, and karyotyping were normal. Fragile X syndrome was excluded by molecular analysis of *FMR1*. A detailed neuropsychological assessment of the affected children and their unaffected brother (V-2) is presented in Table S2.

All together, both families present a clinical phenotype characterized by mild ID and microcephaly (Table 1).

Under the assumption that the causative variant would be homozygous and identical by descent in both children of family 1, homozygosity mapping was performed as described before.[16] The results revealed five candidate regions on chromosomes 1, 5, 11, 12, and 17 for a total length of 63 Mb (Figure S1). Subsequently, exome sequencing of DNA from individual IV-3 was performed as described before.[17] 73.63% of target reads were covered to a depth of 20×, and 83.38% were covered to a depth of at least 5×. A total of 44,955 single-nucleotide variants (SNVs) and 3,140 insertions or deletions (indels) were identified. The candidate regions contained 44 homozygous variants, eight of which were exonic or splice-site variants. Only the homozygous candidate variant in *TAF13* (GenBank: NM_005645.3), c.119T>A (p.Met40Lys), affects a highly conserved residue; it was predicted to be pathogenic by all applied in silico programs and was absent in 380 Syrian control individuals, 728 in-house exomes, and the Exome Aggregation Consortium (ExAC) Browser, NHLBI Exome Sequencing Project (ESP) Exome Variant Server (EVS), and 1000 Genomes (Table S3). Sanger sequencing for all healthy siblings, both affected individuals, and parents proved that the variant in *TAF13* segregates with ID in the family. Re-evaluation of the full variant dataset regardless of the hypothesis of a homozygous causative variant revealed no convincing candidates.

A recessive mode of inheritance was also assumed for family 2. Exome sequencing of family 2 individuals V-1 and V-3 was performed; the average coverage depth was 104×, and >75% of the target nucleotides covered at a minimum of 20×. A total of 24,250 coding variants in V-1 and 23,915 in V-3 were called. Filtering retained high-quality variants that were classified as deleterious (missense, nonsense, indel, and splice-site variants ± 5 bp around exon boundaries) and were not present in the ExAC Browser, EVS, or 1000 Genomes. Assuming a recessive mode of inheritance for the clinical phenotype in the studied family and considering the consanguineous marriage, we compared the exomes of the two affected brothers in a search for shared rare (<0.5% minor allele frequency) homozygous variants. Of the total filtered coding variants identified in the two siblings, homozygous variants were shared in five genes (*EPOR* [MIM: 133171], *KRT15* [MIM: 148030], *SRSF10* [MIM: 605221], *TAF13* [MIM: 600774], and *ZBTB17* [MIM: 604084]). Combined scores of conservation and bioinformatics prediction algorithms highlighted *TAF13* c.92T>A (p.Leu31His), a rare homozygous variant that affects a highly conserved residue and is likely to be pathogenic (Table S3). We performed Sanger confirmation and segregation analysis of this missense variant in the family by genotyping the other two siblings (V-2 and V-4; Figure 1), the parents, and eight additional relatives. The *TAF13* variant was identified in the heterozygous state in seven subjects and co-segregated with the disease phenotype.

To provide further evidence of pathogenicity for the detected variants, we sought to assess their effect by molecular modeling based on the known crystal structure of the TAF13-TAF11 heterodimer. In the TAF13-TAF11 complex, TAF13 forms two α helices connected by a tight turn. This conformation is stabilized by intramolecular interactions formed between the hydrophobic residue pairs Leu31-Ile62 and Met40-Leu57 (Figure 2A, I). In both variants (p.Met40Lys and p.Leu31His), a hydrophobic residue is replaced by a positively charged residue, resulting in a loss of the hydrophobic interactions with Leu57 or Ile62. These structural effects are predicted to destabilize interactions between the α1 and α2 helices of

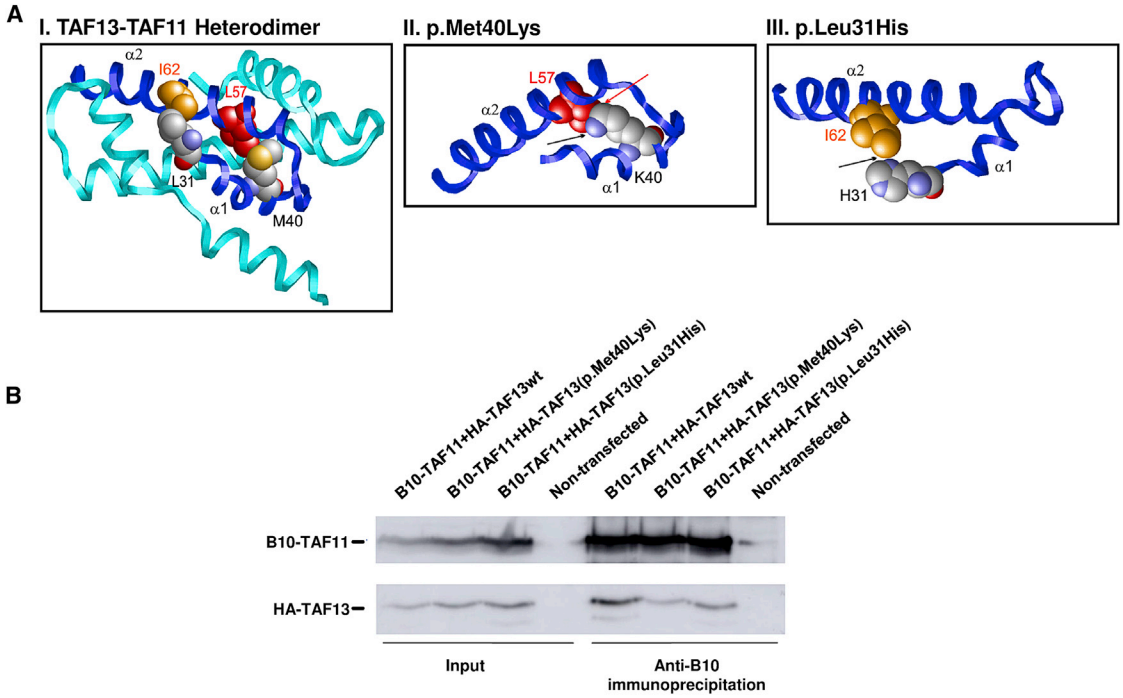

Figure 2. Pathogenicity of TAF13 Variants on the Formation of the TAF13-TAF11 Complex

(A) I: structure of TAF13 (dark blue) in complex with TAF11 (cyan). Residues Leu31 and Met40 are shown in space-filled presentation and colored according to their atom types. The interacting residues Leu57 and Ile62 are colored in red and orange, respectively. II: the p.Met40Lys pathogenic variant results in unfavorable interactions between the Lys40 amide group and the hydrophobic Leu62 side chain (black arrow) and additionally causes steric clashes because the lysine side chain is longer than the methionine (red arrow). III: the p.Leu31His pathogenic variant results in a loss of the hydrophobic contacts with Ile62 (black arrow). In summary, the structural effects described above for the p.Leu31His and p.Met40Lys pathogenic variants destabilize the bent TAF13 conformation required for TAF11 binding and are therefore expected to hamper formation of the TAF13-TAF11 complex. The investigation of the structural effects of the p.Leu31His and p.Met40Lys variants was based on the crystal structure of the TAF13-TAF11 complex (PDB: 1BH8).[3] We modeled mutations with SWISS-Model[18] by selecting the lowest-energy sidechain rotamer for each mutated residue. Structure analysis and visualization was performed with RasMol.[19]

(B) Western blots of coIP experiments of the HeLa cells transfected with TAF11 and either wild-type or mutant TAF13. The anti-B10 antibody (3010F12, provided by the laboratory of Irwin Davidson) was to precipitate TAF11, and TAF13 levels were assessed with an anti-HA antibody (H6908, Sigma).

the TAF13 histone fold (interactions that stabilize the L1 loop required for heterodimerization with TAF11) and are therefore expected to affect formation of the TAF13-TAF11 complex (Figure 2A, II and III).

We next sought to investigate this prediction by using co-immunoprecipitation (coIP). We cloned *TAF13* (wild-type and mutants) into a pCDNA3.1-HA-His vector and *TAF11* into a pAT6 vector, which allows the expression of a B10-epitope-tagged version of TAF11. Then, HeLa cells were transfected with pCDNA3.1-HA-His containing wild-type or mutant *TAF13* and pAT6 containing *TAF11*. CoIP experiments were performed on protein extracted from transfected cells with the anti-B10 antibody to precipitate TAF11-TAF13 complexes, and then immunoblotting was performed with anti-HA antibody to detect co-precipitated TAF13. As shown in Figure 2B, both variants reduced the TAF11-TAF13 interaction such that they led to less precipitation of TAF13 than the wild-type, although comparable amounts of TAF11 were precipitated in all reactions (Figure 2B). The effect was particularly marked with the c.119T>A (p.Met40Lys) variant. In addition to these clinical, genetic, modeling, and biochemical results, the fact that mutations in other components of the TFIID complex (*TAF1*, *TAF2*, *TAF6*, and *TBP*) lead to a neurological phenotype[8–15] strongly supports our hypothesis that bi-allelic pathogenic alterations in the histone fold domain of TAF13 lead to mild ID and microcephaly.

TAF13 is a constituent of at least two protein complexes: the TFIID complex and the small nuclear RNA gene-specific TAF complex (snTAFc), which play a critical role in the regulation of gene transcription in eukaryotic cells.[20,21] To test for the consequences of loss of function of TAF13 on the gene expression pattern, we knocked down 80% of the expression of *TAF13* by using siRNA in human neuroblastoma cells (SK-N-BE; Figure S2A) and subsequent RNA sequencing. Of 21,620 evaluated Ensembl genes, we selected 16,984 with an HGNC gene symbol. Compared with control cells, knockdown cells showed deregulation of 1,278 (7.8%) of these genes ($|\text{fold change}| > 1.5$ and $p < 0.01$; Figures S2B and S2C and Table S4). This strong deregulation of so many genes was also reported after knockdown of a *TAF13* homolog in yeast (*TAF13*)[22] and knockdown of other TAF-encoding genes, *TAF1* and *TAF7* (MIM: 600573), in HEK293 cell lines.[23]

Our analysis using the Molecular Signatures Database (MSigDB) for transcription factor targets[24] revealed significant enrichment of several transcription factor binding motifs, such as the E-box (CANNTG) or other motifs (e.g., AACTTT and CTTTGT), in the genes deregulated by *TAF13* knockdown (Table S5).

Functional enrichment analysis of the 1,278 deregulated genes (DEGs) via Ingenuity Pathway Analysis (IPA) revealed that a broad spectrum of functions were affected, often with an increased activity state (Table S6). This led to the assumption that TAF13 is involved in a wide range of transcription regulations in different tissues and pathways. The top six positions of affected functions were general cell functions of movement, migration, proliferation, morphology, protrusion formation, and differentiation. These were followed by neuron development, neuron proliferation, and neuritogenesis. The seemingly important role of TAF13 in the developmental stages of the CNS also agrees with the increase in *TAF13* expression in fetal brain development (Figure S3A) and during the differentiation of SK-N-BE cells (Figure S3B).

This prompted us to test proliferation and differentiation in SK-N-BE cell lines with *TAF13* knockdown. In the cell-proliferation assay, cells were seeded and transfected with siRNA against *TAF13*. Cells were then counted by colorimetric assay, and *TAF13*-knockdown SK-N-BE cells were found to exhibit a 2-fold higher proliferation rate than negative control cells ($p < 0.0001$; Figure S4), consistent with the increased activation state of the cellular proliferation we obtained from transcriptome sequencing. To study the changes in the differentiation of SK-N-BE cells after *TAF13* knockdown, we induced SK-N-BE cells to form neuronal-like cells by using a mixture of retinoic acid (RA) and caffeic acid (CA)[25] and used quantitative real-time PCR to measure the expression of specific differentiation markers: growth-associated protein 43 (*GAP43* [MIM: 162060]), microtubule-associated protein tau (*MAPT* [MIM: 157140]), and v-myc avian myelocytomatosis viral oncogene neuroblastoma derived homolog (*MYCN* [MIM: 164840]).[26] Expression of *GAP43* and *MAPT* was significantly reduced ($p < 0.0001$) in both differentiating and undifferentiated knockdown SK-N-BE cells. *MYCN* showed no significant change in the undifferentiated cells but was significantly downregulated in the differentiating cells (Figures S3C and S3D). Although we did not achieve a stable knockdown of *TAF13* for the full differentiation process across 12 days,[26] it appears that TAF13 regulates the expression of many genes included in the differentiation process. Furthermore, we performed a migration scratching assay and observed raised migration. However, we cannot reliably distinguish migration from the proliferation effect (data not shown).

Previously, it was reported that TAF13 is involved in transcription regulation as a subunit of the TFIID complex and the snTAFc. Moreover, several lines of evidence suggest that TAF13 has two more domains that are next to the highly conserved histone-fold motif (35–68 aa) and might participate in other protein-protein interactions.[27,28] The diversity of proteins that might interact with TAF13[27,28] and the diversity and intensity of the genes affected by knockdown of *TAF13* suggest a wider functional role than is known at the present time. The pathogenic variants identified here on the basis of molecular modeling and biochemical analysis impair but do not completely abolish TAF11-TAF13 heterodimerization. This possibly explains the viable and rather moderate phenotype of the affected individuals as it compares with the extensive cellular abnormalities observed in the *TAF13*-knockdown SK-N-BE cell lines. Also, the milder effect that we obverted for variant Leu31His (in family 2) in the coIP possibly explains the milder clinical presentation of family 2, particularly the absence of growth retardation and the milder microcephaly. Intriguingly, in other subunits of TFIID, different variants lead to different phenotypes. Variants in TAF1 are associated with ID and microcephaly[13,14] whereas the reduction in *TAF1* expression is associated with XDP[10] (Table S1). Also, in *TBP*, the expansion of the polyglutamine (polyQ) tract causes SCA17 probably in a gain-of-function mode, whereas heterozygous deletion of *TBP* is probably responsible for ID and microcephaly[9,29] (Table S1). Therefore, we also suggest that TAF13 and possibly other constituents of TFIID are multi-functional proteins whose pathogenic variants could lead to different phenotypes depending on the localization of the pathogenic variant. Thus, variants in other domains of TAF13 would not necessarily lead to the same clinical presentation as in the examined individuals in this study.

In conclusion, we suggest that pathogenic bi-allelic variants in *TAF13* cause autosomal-recessive ID with microcephaly. The results of this study suggest an important role for TAF13 and its heterodimerization with TAF11 in neuronal development and brain dysfunction. The multifunctional nature of TAF13 reveals a glimpse of its possible involvement in further clinical phenotypes. A deeper understanding of the molecular mechanisms underlying the structural and functional contribution of TAF13 to the TFIID complex and its gene targets will reveal new insights into many aspects of neurodevelopment and related disorders.

Accession Numbers

ClinVar accession numbers for the variants reported in this paper were not available from ClinVar as of the date this article was finalized for press; please contact the corresponding author for the numbers.

Supplemental Data

Supplemental Data contain four figures and six tables and can be found with this article online at http://dx.doi.org/10.1016/j.ajhg.2017.01.032.

Acknowledgments

We are grateful to the families who participated in this study. We thank Farah Radwan (Human Genetic Institute, Erlangen) for great technical assistance and Dr. Raminder Sing (Translational Research Center, Erlangen) for his help with the cell proliferation assay. This study was supported by the Deutsche Forschungsgemeinschaft (DFG) through grants AB393/2-1 and AB393/2-2 to R.A.J., by the Deutscher Akademischer Austauschdienst (DAAD) through a scholarship to H.T. (A/10/98311), and in part by a grant from Regione Lombardia (Innovative Research Project 1137-2010) to R.C. Work in the Davidson laboratory was supported by grants from the Agence Nationale de la Recherche (ANR-10-LABX-0030-INRT) under the programme Investissements d'Avenir. Intellectual disability is an équipe labellisée of the Ligue Nationale contre le Cancer.

Received: July 8, 2016
Accepted: January 25, 2017
Published: March 2, 2017

Web Resources

1000 Genomes, http://www.1000genomes.org
ClinVar, https://www.ncbi.nlm.nih.gov/clinvar/
Exome Aggregation Consortium (ExAC) Browser, http://exac.broadinstitute.org
Genome Aggregation Database (gnomAD), http://gnomad.broadinstitute.org
MutationTaster, http://www.mutationtaster.org/
NHLBI Exome Sequencing Project (ESP) Exome Variant Server, http://evs.gs.washington.edu/EVS/
OMIM, http://www.omim.org
PolyPhen-2, http://genetics.bwh.harvard.edu/pph2/
RCSB Protein Data Bank, http://www.rcsb.org/
RefSeq, https://www.ncbi.nlm.nih.gov/refseq/
SIFT, http://sift.jcvi.org/
UCSC Genome Browser, http://www.genome.ucsc.edu

References

1. Musante, L., and Ropers, H.H. (2014). Genetics of recessive cognitive disorders. Trends Genet. *30*, 32–39.
2. Reuter, M.S., Tawamie, H., Buchert, R., Hosny Gebril, O., Froukh, T., Thiel, C., Uebe, S., Ekici, A.B., Krumbiegel, M., Zweier, C., et al. (2017). Diagnostic Yield and Novel Candidate Genes by Exome Sequencing in 152 Consanguineous Families With Neurodevelopmental Disorders. JAMA Psychiatry. Published online January 11, 2017. http://dx.doi.org/10.1001/jamapsychiatry.2016.3798.
3. Birck, C., Poch, O., Romier, C., Ruff, M., Mengus, G., Lavigne, A.C., Davidson, I., and Moras, D. (1998). Human TAF(II)28 and TAF(II)18 interact through a histone fold encoded by atypical evolutionary conserved motifs also found in the SPT3 family. Cell *94*, 239–249.
4. Mengus, G., May, M., Jacq, X., Staub, A., Tora, L., Chambon, P., and Davidson, I. (1995). Cloning and characterization of hTAFII18, hTAFII20 and hTAFII28: three subunits of the human transcription factor TFIID. EMBO J. *14*, 1520–1531.
5. Cler, E., Papai, G., Schultz, P., and Davidson, I. (2009). Recent advances in understanding the structure and function of general transcription factor TFIID. Cell. Mol. Life Sci. *66*, 2123–2134.
6. Papai, G., Tripathi, M.K., Ruhlmann, C., Layer, J.H., Weil, P.A., and Schultz, P. (2010). TFIIA and the transactivator Rap1 cooperate to commit TFIID for transcription initiation. Nature *465*, 956–960.
7. Louder, R.K., He, Y., López-Blanco, J.R., Fang, J., Chacón, P., and Nogales, E. (2016). Structure of promoter-bound TFIID and model of human pre-initiation complex assembly. Nature *531*, 604–609.
8. Koide, R., Kobayashi, S., Shimohata, T., Ikeuchi, T., Maruyama, M., Saito, M., Yamada, M., Takahashi, H., and Tsuji, S. (1999). A neurological disease caused by an expanded CAG trinucleotide repeat in the TATA-binding protein gene: a new polyglutamine disease? Hum. Mol. Genet. *8*, 2047–2053.
9. Rooms, L., Reyniers, E., Scheers, S., van Luijk, R., Wauters, J., Van Aerschot, L., Callaerts-Vegh, Z., D'Hooge, R., Mengus, G., Davidson, I., et al. (2006). TBP as a candidate gene for mental retardation in patients with subtelomeric 6q deletions. Eur. J. Hum. Genet. *14*, 1090–1096.
10. Makino, S., Kaji, R., Ando, S., Tomizawa, M., Yasuno, K., Goto, S., Matsumoto, S., Tabuena, M.D., Maranon, E., Dantes, M., et al. (2007). Reduced neuron-specific expression of the TAF1 gene is associated with X-linked dystonia-parkinsonism. Am. J. Hum. Genet. *80*, 393–406.
11. Najmabadi, H., Hu, H., Garshasbi, M., Zemojtel, T., Abedini, S.S., Chen, W., Hosseini, M., Behjati, F., Haas, S., Jamali, P., et al. (2011). Deep sequencing reveals 50 novel genes for recessive cognitive disorders. Nature *478*, 57–63.
12. Hellman-Aharony, S., Smirin-Yosef, P., Halevy, A., Pasmanik-Chor, M., Yeheskel, A., Har-Zahav, A., Maya, I., Straussberg, R., Dahary, D., Haviv, A., et al. (2013). Microcephaly thin corpus callosum intellectual disability syndrome caused by mutated TAF2. Pediatr. Neurol. *49*, 411–416.e1.
13. Hu, H., Haas, S.A., Chelly, J., Van Esch, H., Raynaud, M., de Brouwer, A.P., Weinert, S., Froyen, G., Frints, S.G., Laumonnier, F., et al. (2016). X-exome sequencing of 405 unresolved families identifies seven novel intellectual disability genes. Mol. Psychiatry *21*, 133–148.
14. O'Rawe, J.A., Wu, Y., Dörfel, M.J., Rope, A.F., Au, P.Y., Parboosingh, J.S., Moon, S., Kousi, M., Kosma, K., Smith, C.S., et al. (2015). TAF1 Variants Are Associated with Dysmorphic Features, Intellectual Disability, and Neurological Manifestations. Am. J. Hum. Genet. *97*, 922–932.
15. Yuan, B., Pehlivan, D., Karaca, E., Patel, N., Charng, W.L., Gambin, T., Gonzaga-Jauregui, C., Sutton, V.R., Yesil, G., Bozdogan, S.T., et al. (2015). Global transcriptional disturbances underlie Cornelia de Lange syndrome and related phenotypes. J. Clin. Invest. *125*, 636–651.
16. Abou Jamra, R., Wohlfart, S., Zweier, M., Uebe, S., Priebe, L., Ekici, A., Giesebrecht, S., Abboud, A., Al Khateeb, M.A., Fakher, M., et al. (2011). Homozygosity mapping in 64 Syrian consanguineous families with non-specific intellectual disability reveals 11 novel loci and high heterogeneity. Eur. J. Hum. Genet. *19*, 1161–1166.
17. Riecken, L.B., Tawamie, H., Dornblut, C., Buchert, R., Ismayel, A., Schulz, A., Schumacher, J., Sticht, H., Pohl, K.J., Cui, Y., et al. (2015). Inhibition of RAS activation due to a homozygous ezrin variant in patients with profound intellectual disability. Hum. Mutat. *36*, 270–278.

18. Guex, N., and Peitsch, M.C. (1997). SWISS-MODEL and the Swiss-PdbViewer: an environment for comparative protein modeling. Electrophoresis *18*, 2714–2723.
19. Sayle, R.A., and Milner-White, E.J. (1995). RASMOL: biomolecular graphics for all. Trends Biochem. Sci. *20*, 374.
20. Purrello, M., Di Pietro, C., Viola, A., Rapisarda, A., Stevens, S., Guermah, M., Tao, Y., Bonaiuto, C., Arcidiacono, A., Messina, A., et al. (1998). Genomics and transcription analysis of human TFIID. Oncogene *16*, 1633–1638.
21. Zaborowska, J., Taylor, A., Roeder, R.G., and Murphy, S. (2012). A novel TBP-TAF complex on RNA polymerase II-transcribed snRNA genes. Transcription *3*, 92–104.
22. Shen, W.-C., Bhaumik, S.R., Causton, H.C., Simon, I., Zhu, X., Jennings, E.G., Wang, T.-H., Young, R.A., and Green, M.R. (2003). Systematic analysis of essential yeast TAFs in genome-wide transcription and preinitiation complex assembly. EMBO J. *22*, 3395–3402.
23. Devaiah, B.N., Lu, H., Gegonne, A., Sercan, Z., Zhang, H., Clifford, R.J., Lee, M.P., and Singer, D.S. (2010). Novel functions for TAF7, a regulator of TAF1-independent transcription. J. Biol. Chem. *285*, 38772–38780.
24. Subramanian, A., Tamayo, P., Mootha, V.K., Mukherjee, S., Ebert, B.L., Gillette, M.A., Paulovich, A., Pomeroy, S.L., Golub, T.R., Lander, E.S., and Mesirov, J.P. (2005). Gene set enrichment analysis: a knowledge-based approach for interpreting genome-wide expression profiles. Proc. Natl. Acad. Sci. USA *102*, 15545–15550.
25. Chlapek, P., Redova, M., Zitterbart, K., Hermanova, M., Sterba, J., and Veselska, R. (2010). Enhancement of ATRA-induced differentiation of neuroblastoma cells with LOX/COX inhibitors: an expression profiling study. J. Exp. Clin. Cancer Res. *29*, 45.
26. Leotta, C.G., Federico, C., Brundo, M.V., Tosi, S., and Saccone, S. (2014). HLXB9 gene expression, and nuclear location during in vitro neuronal differentiation in the SK-N-BE neuroblastoma cell line. PLoS ONE *9*, e105481.
27. Jeronimo, C., Forget, D., Bouchard, A., Li, Q., Chua, G., Poitras, C., Thérien, C., Bergeron, D., Bourassa, S., Greenblatt, J., et al. (2007). Systematic analysis of the protein interaction network for the human transcription machinery reveals the identity of the 7SK capping enzyme. Mol. Cell *27*, 262–274.
28. Havugimana, P.C., Hart, G.T., Nepusz, T., Yang, H., Turinsky, A.L., Li, Z., Wang, P.I., Boutz, D.R., Fong, V., Phanse, S., et al. (2012). A census of human soluble protein complexes. Cell *150*, 1068–1081.
29. Eash, D., Waggoner, D., Chung, J., Stevenson, D., and Martin, C.L. (2005). Calibration of 6q subtelomere deletions to define genotype/phenotype correlations. Clin. Genet. *67*, 396–403.